ISBN: 978-3-95450-208-0 doi:10.18429/JACoW-IPAC2019-TUPTS070

# SYSTEMATIC BENCHMARKING OF A PLANAR (N)UNCD FIELD EMISSION CATHODE

J. Shao[1,*], G. Chen[2], M. Schneider[3], K. Kovi[4], L. Spentzouris[2], E. Wisniewski[1], J. Power[1], M. Conde[1], W. Liu[1], S. Baryshev[3†]
[1]Argonne National Laboratory, Lemont, IL 60439, USA
[2]Illinois Institute of Technology, Chicago, IL 60616, USA
[3]Michigan State University, East Lansing, MI 48824, USA
[4]Euclid Techlabs LLC, Bolingbrook, IL 60440, USA

*Abstract*

Planar nitrogen-incorporated ultrananocrystalline diamond, (N)UNCD, is a unique and attractive field emission source because of the capability to generate high charge beam, the simplicity of production without shaped emitters, and the ease of handling with moderate vacuum requirement. In the presented study using an L-band normal conducting single-cell rf gun, a (N)UNCD cathode has been conditioned to 42 MV/m with a well-controlled manner and reached a maximum charge of 15 nC and an average emission current of 6 mA during a 2.5 µs emission period. The systematic study of emission properties during the rf conditioning process illustrates the tunability of (N)UNCD in a wide range of surface gradients. This research demonstrates the versatility of (N)UNCD cathode which could enable multiple designs of field emission rf injector for industrial and scientific applications.

## INTRODUCTION

The planar UNCD cathode is an attractive field emission (FE) electron source because of its simplicity and scalability to fabricate and to obtain high current without the requirement of pre-defined or shaped emitters [1–3] This is supported by the fact that emission current of planar diamond comes from grain boundaries [4] and UNCD enjoys the highest grain boundary density within the diamond cathode family. In addition, the planar UNCD cathode is robust to electric field with moderate vacuum requirement (at the order of $10^{-8}$ Torr). To date, planar UNCD cathodes have been successfully tested at 20-70 MV/m in normal conducting rf guns [1, 2], at 1 MV/m under cryogenic temperatures of 2-4 K in a superconducting rf gun [5], and at 1-20 MV/m in dc setups [3].

This work extends the characterization of UNCD cathodes from a fixed electric field level to various levels during the rf conditioning process. Detailed emission properties, including current, field enhancement factor $\beta$, effective emission area $A_e$, microscopic maximum electric field, current density, longevity, have been recorded as the macroscopic field was pushed from 8 MV/m to 42 MV/m in a well-controlled conditioning process. This study demonstrates the versatility of planar UNCD cathode and provides large parameters space for realistic FE-based injector design.

## CATHODE PREPARATION

The cathode plug (28 mm tall and 20 mm in diameter) is designed as a three-part assembly with an aluminum body, an aluminum middle piece, and a stainless steal top piece, as illustrated in Fig. 1. The design meets the installation requirements of the L-band photocathode rf gun test-stand [2, 6, 7] and enables convenient material synthesis onto the thin top part. The parts are aligned with each other and assembled together using internal vented screws. The electrical contact between the cathode assembly and the rf gun is ensured by a spring around the cathode body.

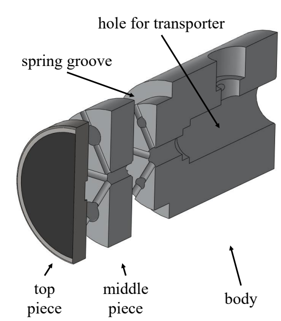


Figure 1: Cross section of the cathode assembly. The dark part of the top piece represents the (N)UNCD material. The vented screws holding the parts are not shown.

The top piece was first coated with a buffer molybdenum layer. Then the (N)UNCD material was deposited on top of it using the microwave-assisted plasma chemical vapor deposition method [8]. The area covered by (N)UNCD was 18 mm in diameter.

## EXPERIMENTAL SETUP

The experiment was conducted on the Argonne Cathode Test-stand (ACT) beamline at the Argonne Wakefield Accelerator (AWA) facility [2, 6, 7], as illustrated in Fig. 2. The ACT beamline equips with a single-cell normal conducting photocathode rf gun operated at L-band 1.3 GHz. The beamline currently runs at 2 Hz repetition with a full width half maximum (FWHM) pulse length of 6 µs. ~227 W input power is required to obtain 1 MV/m electric field on the flat

* jshao@anl.gov
† serbar@msu.edu

ISBN: 978-3-95450-208-0 doi:10.18429/JACoW-IPAC2019-TUPTS070



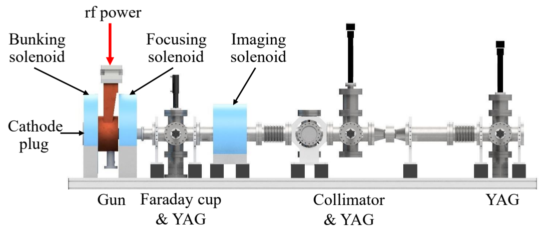


Figure 2: Layout of the ACT beamline at AWA.

Diagnostics involved in the experiment include a direction coupler to monitor the input and reflection rf power, an rf pickup installed at the gun side-wall to detect the field profile, an aluminum block acting as a Faraday cup at the gun exit to collect the field emission current, and YAG screens to observe the beam transverse profile along the beamline. A photomultiplier tube (PMT) with a fluorescent screen sensitive to X-ray was placed near the gun for machine inter-lock in the event of rf breakdown. The strength of the focusing solenoid (denoted as $B_f$) was used to maximize the electron beam capture ratio by the Faraday cup.

## EXPERIMENTAL RESULT

The macroscopic electric field on the cathode $E_c$ and the average emission current $\overline{I_F}$ are illustrated in Fig. 3. The profile of the emission current is approximated as a square pulse for simplicity in the following data analysis. The square pulse has an amplitude of $\overline{I_{F,\max}}$ and its width depends on the maximum microscopic electric field (defined as the product of the maximum macroscopic electric field during the rf pulse $E_{c,\max}$ and $\beta$), as illustrated in the inset of Fig. 3.

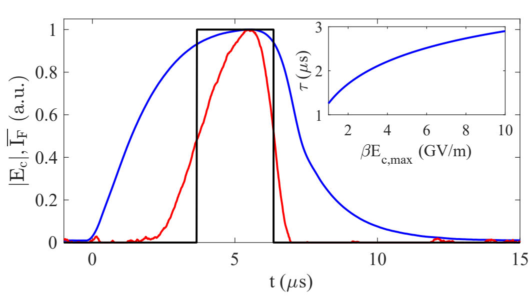


Figure 3: Blue: the normalized cathode field amplitude measured by the rf pickup. Red: the average emission current measured by the Faraday cup. Black: the square pulse approximation of the emission profile. Inset: The width of the square emission profile as a function of $\beta E_{c,\max}$.

Due to the detachable cathode design, field emission electrons may come from the edge of the cathode/insertion hole other than the cathode itself. The two sources can not be distinguished by the Faraday cup. Therefore, a YAG screen at the same location (denoted as $YAG_1$) as the Faraday cup was used to evaluate the emission current from these sources.

Figure 4(a) illustrates the ASTRA simulation results of the YAG image when there are six field emitters (each with 0.2 mm diameter) on the cathode edge. The line-shaped pattern is caused by the wide energy spread of the field emission current. In the experimental using the (N)UNCD cathode with the same $E_{c,\max}$ and $B_f$, the similar shape and location of a bright line (marked by the red circle in Fig. 4(b)) as simulation suggests that there was one edge emitter. The rest bright lines in the observed pattern are caused by emitters on the (N)UNCD material, whose total brightness is much higher than that of the edge emitter. Therefore, the collected charge was dominated by emitters on the (N)UNCD material. In comparison, the experimental result using a molybdenum cathode without (N)UNCD material is illustrated in Fig. 4(c), which clearly shows that the emission was mainly from edge emitters.

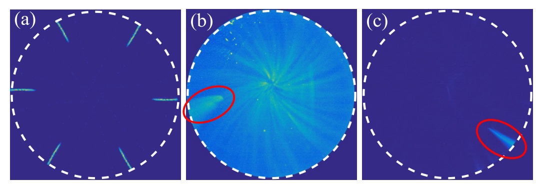


Figure 4: Simulated transverse distribution of six edge emitters on $YAG_1$ (a), and comparison of experimental results using the (N)UNCD cathode (b) and a molybdenum cathode (c). The images were simulated or taken with the same $E_{c,\max}$ and $B_f$ settings. The white dashed circles represent the YAG boundary (44 mm in diameter). The red circles mark edge emitters.

$E_{c,\max}$ has been gradually increased from 8 MV/m to 42 MV/m to study the (N)UNCD field emission properties during rf conditioning. In the conditioning process, the increment of $E_{c,\max}$ was ~0.5 MV/m. The breakdown rate could be as high as $1 \times 10^{-1}$ /pulse immediately after the increment. Before the next increase, $E_{c,\max}$ was kept at the same level until the breakdown rate decreased to $1 \times 10^{-3}$. When continuous breakdown occurred, the field was reduced to a much lower level until no breakdown happened and then pushed back. The entire rf conditioning and measurements lasted for 40 hours.

When conditioned to certain $E_{c,\max}$ levels, e.g. 20 MV/m, 40 MV/m, etc., $E_{c,\max}$ was kept until the rf breakdown rate dropped below $5 \times 10^{-4}$. Then $E_{c,\max}$ was gradually decreased and the corresponding charge was recorded in order to fit $\beta$ and $A_e$ according to the Fowler-Nordheim (F-N) equation [9], as illustrated in Fig. 5. The good linearity in the F-N coordinate suggests the emission was not space-charge limited [10]. It can be seen that $\overline{I_{F,\max}}$ for a fixed field level kept decreasing during rf conditioning. Meanwhile, the maximum achievable $\overline{I_{F,\max}}$ first increased, reached ~6 mA at $E_{c,\max}$=36 MV/m, then dropped to ~5 mA at $E_{c,\max}$=42 MV/m.

The fitted emission properties during rf conditioning are illustrated in Fig. 6. In the figure, $E_h$ and $\overline{I_h}$ denote the highest achieved $E_{c,\max}$ and the corresponding $\overline{I_{F,\max}}$, respectively.

ISBN: 978-3-95450-208-0 doi:10.18429/JACoW-IPAC2019-TUPTS070

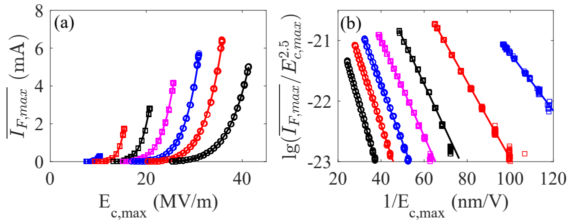


Figure 5: The dependence of $\overline{I_{F,\max}}$ on $E_{c,\max}$, plotted in the $E_{c,\max} - \overline{I_{F,\max}}$ coordinate (a) and the F-N coordinate (b). The dots denote the experimental data and the lines represent the linear fitting results from the F-N coordinate.

$\beta$ kept decreasing during the rf conditioning while the maximum microscopic field level $\beta E_h$ first increased and then stayed at a fixed value of ~7.5 GV/m. This value agree with the one in a previous study where $E_h$ reached ~70 MV/m [2]. $A_e$ decreased by one order of magnitude to $1 \times 10^4$ nm$^2$ and the current density reached $4.5 \times 10^{11}$ A/m$^2$. A theoretical model is under development to interpret the evolution of the emission properties.

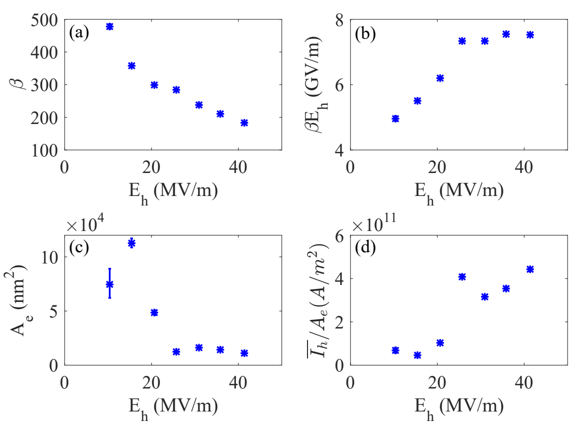


Figure 6: Evolution of field emission properties during rf conditioning. (a) The field enhancement factor; (b) The maximum microscopic electric field; (c) The effective emission area; (d) The current density.

The longevity of the (N)UNCD cathode was tested when $E_{c,\max}$ reached 42 MV/m. In the 4-hour measurement at the highest achievable field level, ~ $3\times10^4$ rf pulses or ~ $1\times10^8$ rf cycles (calculated from the 2.5 µs square emission pulse and the 1.3 GHz operation frequency) were accumulated and the current dropped by only ~4 %, as illustrated in Fig. 7. There were only one breakdown occurred during the measurement. The good longevity and low rf breakdown rate ($3 \times 10^{-5}$ /pulse) demonstrate the promising potential of (N)UNCD material in injector applications.

The field emission properties was measured before and after the 4-hour measurement and the difference is negligible, as illustrated in Fig. 8. Together with the significant variation during rf conditioning, it suggests that the evolution of the field emission properties was mainly caused by rf breakdowns rather than accumulated rf pulses.

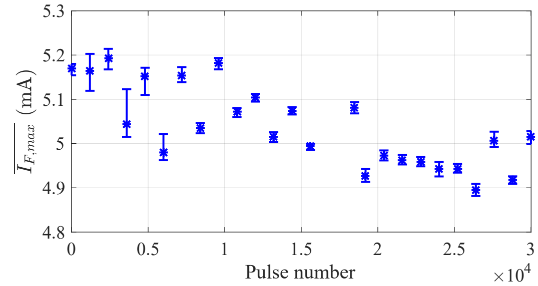


Figure 7: The emission current evolution during the 4-hour longevity measurement.

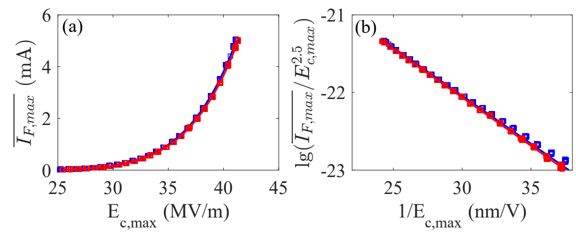


Figure 8: The dependence of $\overline{I_{F,\max}}$ on $E_{c,\max}$ before (blue) and after (red) the longevity measurement, plotted in the $E_{c,\max} - \overline{I_{F,\max}}$ coordinate (a) and the F-N coordinate (b). The dots denote the experimental data and the lines represent the linear fitting results from the F-N coordinate.

## CONCLUSION

This study systematically benchmarked the field emission properties of a planar nitrogen-incorporated ultrananocrystalline diamond during the rf conditioning process where the macroscopic filed was pushed from 8 MV/m to 42 MV/m. The cathode reached a maximum charge of 15 nC and an average emission current of 6 mA during a 2.5 µs emission period. The charge dropped by only ~4 % during a 4-hour longevity measurement at 42 MV/m where ~ $3 \times 10^4$ rf pulses or ~ $1 \times 10^8$ rf cycles were accumulated. This study demonstrates the good potential of (N)UNCD cathodes to be applied in FE-based injectors. In the future, we plan to study the emittance of (N)UNCD field emission cathode and design electron sources based on the parameter space reported in this manuscript.

## ACKNOWLEDGMENT

The work at AWA is funded through the U.S. Department of Energy Office of Science under Contract No. DE-AC02-06CH11357. This work by M. Schneider is supported by the US Department of Energy, Office of Science, High Energy Physics under Cooperative Agreement award number DE-SC0018362 and Michigan State University. The work by S. Baryshev is funded from the College of Engineering, Michigan State University, under the Global Impact Initiative. We would like to thank Dr. Evgenya Simakov at Los Alamos National Laboratory for providing the molybdenum cathode.

ISBN: 978-3-95450-208-0 doi:10.18429/JACoW-IPAC2019-TUPTS070



## REFERENCES


[1] X. Li *et al.*, "Cold cathode rf guns based study on field emission", *Physical Review Special Topics-Accelerators and Beams* vol. 16, p. 123401, 2013.

[2] S. Baryshev *et al.*, "Planar ultrananocrystalline diamond field emitter in accelerator radio frequency electron injector: Performance metrics", *Applied Physics Letters*, vol. 105, p. 203505, 2014.

[3] O. Chubenko *et al.*, "Locally resolved electron emission area and unified view of field emission from ultrananocrystalline diamond films", *ACS Applied materials & Interfaces* vol. 9, pp. 33229–33237, 2017.

[4] V. Chatterjee *et al.*, "Direct observation of electron emission from the grain boundaries of chemical vapour deposition diamond films by tunneling atomic force microscopy", *Applied Physics Letters*, vol. 104, p. 171907, 2014.

[5] Private communication with Dr. Erdong Wang at Brookhaven National Laboratory.

[6] J. Shao *et al.*, "Observation of field-emission dependence on stored energy", *Physical Review Letters*, vol. 115, p. 264802, 2015.

[7] J. Shao *et al.*, "In situ observation of dark current emission in a high gradient rf photocathode gun", *Physical Review Letters*, vol. 117, p. 084801, 2016.

[8] J. Butler *et al.*, "The CVD of nanodiamond materials", *Chemical Vapor Deposition*, vol. 14, pp. 145–160, 2008.

[9] J. Wang and G. Loew, "Field emission and rf breakdown in high-gradient room temperature linac structures", SLAC, Menlo Park, USA, Tech. Rep. SLAC-PUB-7684, 1997.

[10] A. Rokhlenko *et al.*, "Space charge effects in field emission: One dimensional theory", *Applied Physics Letters*, vol. 107, p. 014904, 2010.